# Quantum-interference-enhanced deep sub-Doppler cooling of $^{39}$K atoms in gray molasses

Dipankar Nath,* R Kollengode Easwaran, G. Rajalakshmi, and C. S. Unnikrishnan†
*Tata Institute of Fundamental Research, Navy Nagar, Colaba, Mumbai 400005, India*
(Received 24 May 2013; revised manuscript received 27 August 2013; published 8 November 2013)

We report enhanced sub-Doppler cooling of the bosonic atoms of $^{39}$K facilitated by formation of dark states with the cooling and repumping lasers tuned to the Raman resonance in $\Lambda$ configuration near the $D_1$ transition. A temperature of about 12 $\mu$K and phase-space density $>2\times10^{-5}$ is achieved in the two-stage $D_2$-$D_1$ molasses and spans a very large parameter region where quantum interference persists robustly. We also present results on enhanced radiation heating with a subnatural linewidth ($0.07\Gamma$) and a signature Fano-like profile of a coherently driven three-level atomic system. The optical Bloch equations relevant for the three-level atom in a bichromatic light field are solved with the method of continued fractions to show that cooling occurs only for a small velocity class of atoms, emphasizing the need for precooling in the $D_2$ molasses stage.

DOI: 10.1103/PhysRevA.88.053407 PACS number(s): 37.10.De, 32.80.Wr, 67.85.−d

## I. INTRODUCTION

Potassium and lithium are important alkali-metal-group atoms for a variety of experiments employing cold atoms due to the existence of both fermionic and bosonic isotopes. However, laser cooling of their bosonic isotopes to sub-Doppler temperatures is difficult due to the closely spaced hyperfine levels in the cooling transitions. Further, their evaporative cooling to degeneracy is complicated because of their unfavorable scattering properties. The latter issue is usually solved with either sympathetic cooling with other atoms like rubidium [1,2] or using Feshbach resonances tuned with a magnetic field in an optical trap [3]. To attain sub-Doppler temperatures in $^{39}$K, multistage molasses cooling strategies with relatively large laser power and large detuning in the first stage have to be implemented, yet the lowest temperatures are almost 100 times larger than the recoil limit, compared to a factor of 10 in the case of rubidium. $^{39}$K has been cooled to temperatures as low as 30–40 $\mu$K using $D_2$-line molasses cooling [4–6].

Gray molasses aided by the formation of an optically pumped dark state, with lasers tuned above the $D_1$ line (blue detuning) of the alkali atoms, has been shown to result in ultralow sub-Doppler temperatures [7,8]. Very recently, enhanced cooling due to quantum interference effects and coherent dark-state formation in the Raman configuration involving two driving light modes and a three-level atom have been reported in laser cooling of $^{40}$K [9] and $^{7}$Li [10]. Similar three-level systems have also been used for velocity-selective coherent population trapping (VSCPT) to cool atoms to subrecoil temperatures [11]. In the case of lithium, cooling below the Doppler limit is difficult without the use of a special procedure, like cooling with the narrow $^2S_{1/2}\rightarrow{}^3P_{3/2}$ transition in the UV [12].

While sub-Doppler cooling occurs naturally in $^{40}$K during the standard $D_2$ molasses [5], as its excited-state hyperfine structure is well spaced, this is not true for $^{39}$K, which requires special schemes for sub-Doppler cooling [4–6,13]. We have been working on gray molasses with lasers tuned near the $D_1$ line on $^{39}$K atoms that are precooled in a $D_2$ conventional molasses (see Fig. 1) and have observed that apart from optically pumped dark states aiding the sub-Doppler cooling by a factor of 2–3, quantum interference and coherent dark-state formation helps to achieve sub-Doppler temperatures a further factor of 3 lower, over a very wide detuning range relative to both $F'=2$ and $F'=1$ $D_1$ lines (see Fig. 1).

While the exact Raman configuration always leads to enhanced cooling, there are regions of relative detuning of the cooling and repumping lasers where strong heating of the atomic cloud is observed. The heating follows an asymmetric Fano-like profile with a subnatural linewidth ($<0.1\Gamma$), indicating the presence of a long-lived dressed state. The high reproducibility of the cooling and heating features and the vast parameter region over which the effects persist provide a new test system for the study of the interplay between sub-Doppler laser cooling and quantum interference effects. Unlike the case of gray molasses cooling in $^{40}$K [9] and $^{7}$Li [10], the repump intensity $I_R$ needs to be comparable to that of the cooling intensity $I_C$ for $^{39}$K. However, we still achieve similar cooling efficiencies in $^{39}$K by precooling the atoms to below 100 $\mu$K in a standard $D_2$ molasses cooling [4–6] prior to the $D_1$ (gray) molasses stage. In the rest of the paper, we report the main experimental results and their analysis, especially the ultralow temperatures achieved in the molasses and the Fano-like profiles with subnatural linewidth in radiation heating. We explain some of the observed phenomenon based on coherent-population-trapping effects in a three-level atom driven by two laser fields in the $\Lambda$ configuration. A model for the cooling mechanism in a bichromatic standing-wave light field is developed by solving the optical Bloch equations by the method of continued fractions [14].

## II. EXPERIMENT AND RESULTS

The magneto-optical trap (MOT) is formed using a 767-nm laser tuned below the $D_2$ transition of $^{39}$K atoms. Details of our experimental setup are described in [5]. The cooling and repump beams are derived from the same laser using acousto-optic modulators (AOMs) and then mixed and amplified in a commercially available tapered amplifier (Toptica BoosTA; see Fig. 2). The MOT beams are in the $\sigma_+$-$\sigma_-$ configuration. To capture the atoms in the MOT efficiently, the cooling

*dip@tifr.res.in
†unni@tifr.res.in

 

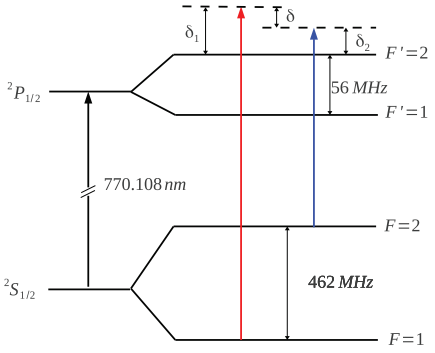


FIG. 1. (Color online) $D_1$ line of $^{39}$K. $\delta_1$ and $\delta_2$ are the repump ($F = 1 \rightarrow F' = 2$) and cooling ($F = 2 \rightarrow F' = 2$) detunings, and $\delta = \delta_1 - \delta_2$ is the relative detuning between the repump and cooling beams.

beam is kept detuned by $-24$ MHz from the $F = 2 \rightarrow F' = 3$ transition and the repump laser is detuned by $-14$ MHz from $F = 1 \rightarrow F' = 2$. We capture about $1 \times 10^8$ atoms in the MOT at a temperature of about 1 mK. The atoms are then put through a compressed-MOT (C-MOT) stage during which the magnetic field is ramped up and the cooling laser detuning is increased to $-42$ MHz. At the end of this stage the density of the trapped atoms is enhanced, but the atoms are heated to temperatures >5 mK. Precooling of these atoms in a $D_2$ sub-Doppler phase reduces their temperature to 40 $\mu$K [5]. The $D_2$ molasses cooling lasts for about 4 ms, and during this phase the detuning of the cooling beam is reduced to $-10$ MHz and that of the repump beam to $-11$ MHz.

The $D_1$ molasses beams are prepared in the following manner. A laser (Toptica DLPro) is tuned to 770.1 nm; a small portion of its power is used for spectroscopy and frequency locking, and the rest is coupled to a homemade tapered amplifier. The "cooling laser" for the $D_1$ $\Lambda$ molasses is near the $F = 2 \rightarrow F' = 2$ transition with detuning $\delta_2$, and the "repump laser" is near the $F = 1 \rightarrow F' = 2$ transition with detuning $\delta_1$. The cooling and repump beams are derived from the output of the tapered amplifier using AOMs, and the relative detuning $\delta = \delta_1 - \delta_2$ and the absolute detuning $\Delta$ from

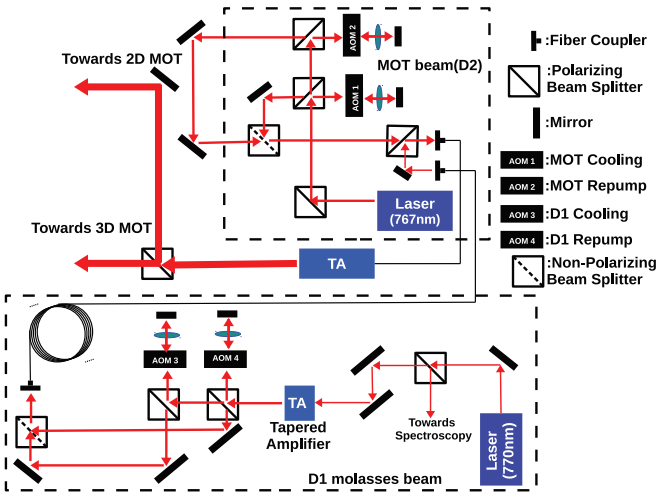


FIG. 2. (Color online) Optical layout for the preparation of cooling and repump beams for addressing $D_1$ and $D_2$ transitions.

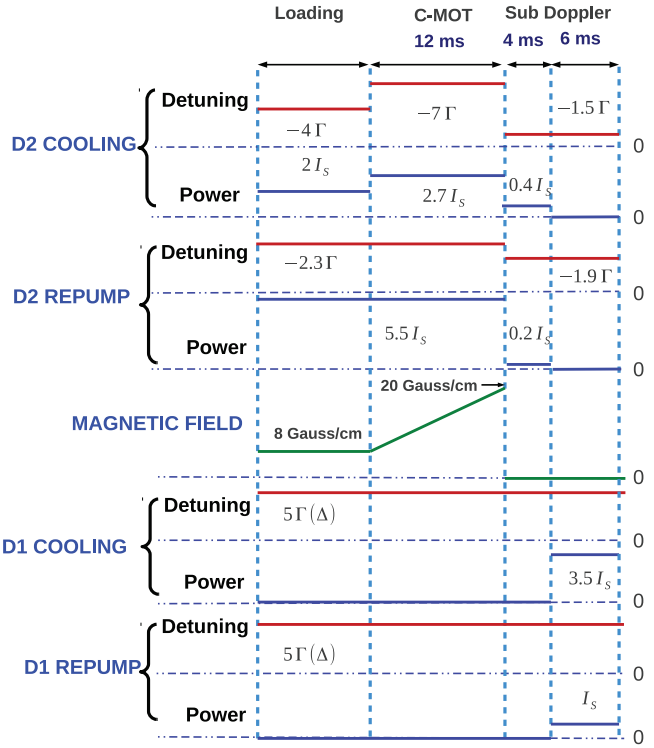


FIG. 3. (Color online) Timing diagram of C-MOT and $D_2$-$D_1$ sub-Doppler cooling phases.

the $D_1$ $F' = 2$ line (when $\delta = 0$) are tunable over a wide range. The cooling and the repump beams thus obtained are mixed and then amplified using the same tapered amplifier used for generating the MOT beams (see Fig. 2). This configuration reduces the additional optics required to produce the six beams for $D_1$ molasses as they are obtained from the same tapered amplifier used to generate the MOT beams, eliminating the need for further optical alignment. Thus the polarization of the $D_1$ molasses beams is same as that of the standard MOT beams; that is, they are in the $\sigma_+$-$\sigma_-$ configuration as in the case of $^7$Li [10].

The $D_1$ beams are switched on immediately after the $D_2$ sub-Doppler phase (see Fig. 3). This second $D_1$ sub-Doppler phase cools the atoms by another factor of 4 or so in the optimal case of the parameter range we explored, down to about 12 $\mu$K without loss of atoms. We achieve the lowest temperatures over a wide range of blue detuning $\Delta$ of the cooling and the repump beams from the $F = 2 \rightarrow F' = 2$ transition.

Although we observe that cooling beyond the $D_2$ molasses occurs over a range of relative detuning $\delta$, extending $\pm 2\Gamma$ around $\delta = 0$, the deepest cooling occurs when the Raman resonance $\delta = 0$ is satisfied. Figure 4 (with $\Delta = 28$ MHz) indicates how the resonant cooling occurs in a very narrow band ($\ll\Gamma$) around the Raman resonance. The intensity ratio between the cooling ($I_c$) and repump ($I_r$) beams is about 3 for optimum cooling, which is much smaller than the ratio used in the case of $^7$Li [10]. For larger ratios of $I_c/I_r$ the cooling is less efficient. A temperature as low as 12 $\mu$K is observed at the Raman resonance. For small positive values of the difference in the detuning $\delta = \delta_1 - \delta_2$ we see strong heating. The heating is almost divergent by a factor of 1000 to temperatures beyond 10 mK and has a width of less than $0.1\Gamma$. The asymmetric Fano

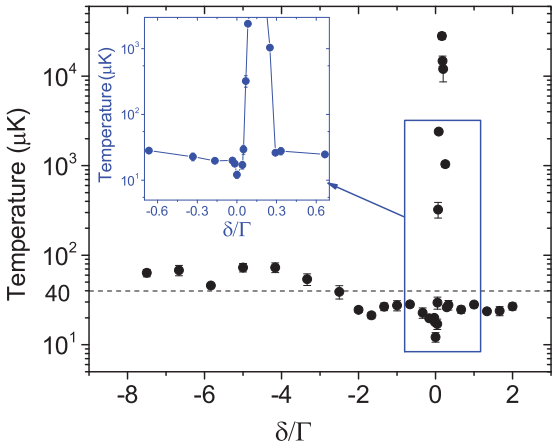


FIG. 4. (Color online) Temperature is measured for various values of the relative detuning $\delta$ around the Raman resonance for $\delta_2 = 28$ MHz. The line at 40 $\mu$K represents the starting temperature for the $D_1$ sub-Doppler phase.

profile, typical of excitation probability in such atomic systems with interfering excitation pathways [15], is visible clearly in detailed measurements, as shown in the inset of Fig. 4.

The two lasers driving the transitions in our experiments on $D_1$ $\Lambda$ dark-state cooling have an intensity ratio $I_c/I_r = (\Omega_2/\Omega_1)^2 \simeq 3.5$ when these parameters are optimized for the best sub-Doppler cooling. This has significant implications on the exact nature of the dark-state formation. If we invert the intensity ratio, i.e., make repump stronger than cooling, the Fano profile shifts sides and appears at $\delta < 0$ (Fig. 5), confirming the role of coherent population trapping in the light scattering as explained in Sec. III. Although the extra sub-Doppler cooling at the Raman resonance and the heating are not as effective here as in the case of $I_c/I_r > 1$, the general trend is clear. Additional cooling happens at the Raman resonance, and strong resonant heating to several mK occurs in a narrow range of $\delta < 0$ close to the Raman resonance, with a width much smaller than $\Gamma$. At all other detunings, we observe mild heating.

The molasses cooling in Raman configuration is effective over a wide range of absolute detuning ($\Delta = \delta_1 = \delta_2$) from the atomic transition, as can be seen from Fig. 6. Over a

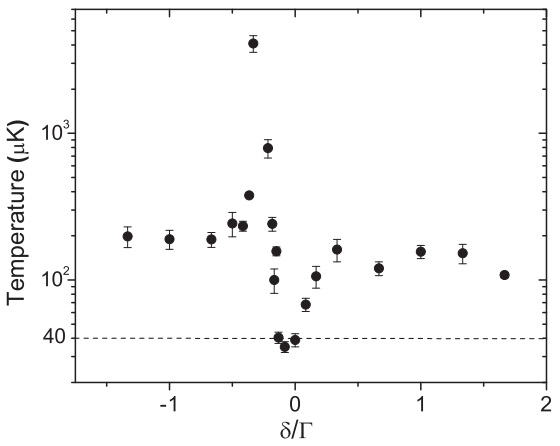


FIG. 5. Temperature vs relative detuning $\delta$ for $I_C/I_R = 0.28$.

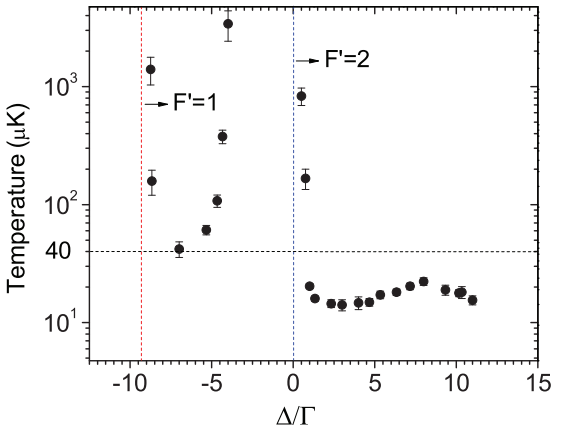


FIG. 6. (Color online) Temperature as a function of the detuning from $F' = 2$ in the Raman configuration ($\Delta = \delta_2 = \delta_1$).

range of $\Delta \approx (60, 10)$ MHz, the quantum coherence-enhanced cooling is relatively independent of the value of $\Delta$. Strong heating takes over at $F' = 2$ resonance and persists until $\Delta \approx -42$ MHz from the $F' = 2$ line, below which we recover the temperatures reached in the $D_2$ sub-Doppler cooling for a small range of detuning. When the lasers are tuned between $F' = 1$ and $F' = 2$, preserving the Raman resonance condition, two $\Lambda$ configurations become operational in the atom, namely, the transitions ($F = 1 \rightarrow F' = 2, F = 2 \rightarrow F' = 2$) and ($F = 1 \rightarrow F' = 1, F = 2 \rightarrow F' = 1$). Clearly, the model for cooling or heating based on the three-level $\Lambda$ configuration will not be adequate, and the opposing contributions from the two configurations largely explain the behavior in Fig. 6. (See Sec. III for a discussion of the model.)

Figure 7 shows the variation of temperature with $I_C/I_R$. As we can see, the cooling is most effective when the value of $I_C/I_R$ lies between 3 and 4. More than 90% of the atoms remain after the $D_2$-$D_1$ molasses cooling scheme.

At the lowest temperature attained, i.e., at 12 $\mu$K, the average density of the atoms in the MOT is about $5 \times 10^{10}/\text{cm}^3$. This corresponds to a phase-space density greater than $2 \times 10^{-5}$ [16].

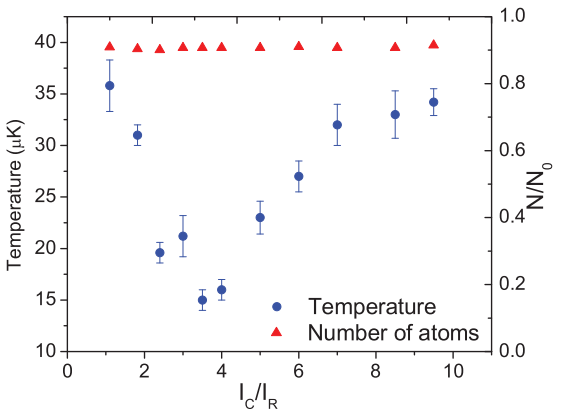


FIG. 7. (Color online) Temperature and fraction of atoms remaining in the cold cloud as a function of various values of cooling to repump intensity. $N_0 = 10^8$ is the atom number prior to the molasses cooling stages.

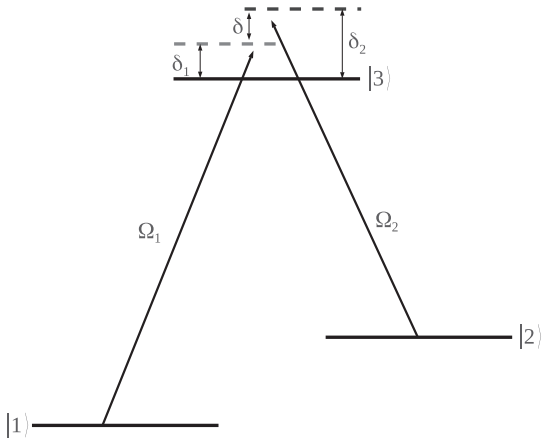


FIG. 8. A model three level Λ−system. $\Omega_1$ & $\Omega_2$ are the Rabi frequencies of the transitions $|1\rangle \rightarrow |3\rangle$ & $|2\rangle \rightarrow |3\rangle$ respectively. $\delta_1$ & $\delta_2$ are the respective detuning and $\delta = \delta_1 - \delta_2$ is the relative detuning.

## III. MODEL FOR COOLING

The enhanced cooling and the other main features in our results can be understood based on the absorption properties of a three-level atomic system in the presence of Λ-type coherent drive fields. Referring to Fig. 8, the levels which correspond to the three-level system in the Λ configuration are formed by the hyperfine ground states $F = 1$ ($|1\rangle$) and $F = 2$ ($|2\rangle$) and the upper hyperfine $D_1$ level $F' = 2$ ($|3\rangle$). The transitions $|1\rangle \rightarrow |3\rangle$ and $|2\rangle \rightarrow |3\rangle$ are excited by laser light with frequencies $\omega_1$ and $\omega_2$, respectively, both in the standing-wave configuration.

Assuming that the two frequencies are almost similar, i.e., $\omega_1 \sim \omega_2 = \omega$, we can write the interaction part of the Hamiltonian of the combined atom-light system as

$$\begin{aligned} H = {} & \hbar\Omega_1 \cos(kz)(|1\rangle\langle 3| + \text{H.c.} \\ & + \hbar\Omega_2 \cos(kz + \phi)(|2\rangle\langle 3| + \text{H.c.} \\ & + \hbar\delta_1 |1\rangle\langle 1| + \hbar\delta_2 |2\rangle\langle 2|. \end{aligned} \tag{1}$$

In the Raman condition ($\delta_1 = \delta_2$) coherent population trapping occurs in a Λ system [11]. It is well known that the Raman condition leads to the formation of a "dark" state which does not couple to any other state. This noncoupling state is given by [17,18]

$$|D\rangle = (\Omega_2|1\rangle - \Omega_1|2\rangle)/\left(\Omega_1^2 + \Omega_2^2\right). \tag{2}$$

In the Raman condition, the atoms will occupy the noncoupling dark state $|D\rangle$, resulting in reduced photon scattering from the atoms. However, the atoms can still couple to the other "bright" states via motional coupling [17]. Atoms transferred to the bright state will sample a periodic variation of Stark shift as they traverse through the standing waves before being pumped back to the dark state. For positive (blue) detuning relative to the $D_1$ transition, the Stark shift results in a periodic pattern of potential humps. Thus a Sisyphus-like mechanism will ensue, which results in cooling of the atoms [17].

The bright states under the approximation $\Omega_1 \ll \Omega_2$ are given by [19]

$$\begin{aligned} |2'\rangle &= \cos\theta\ |2\rangle - \sin\theta\ |3\rangle, \\ |3'\rangle &= \sin\theta\ |2\rangle + \cos\theta\ |3\rangle, \end{aligned} \tag{3}$$

where $\tan 2\theta = \Omega_2/\delta_2$. The linewidths of both these states are predominantly decided by the coefficient of $|3\rangle$ since state $|2\rangle$ has an infinite lifetime and hence has a zero natural linewidth. Thus the linewidths of the two new states are $\Gamma_{|2'\rangle} \sim \sin^2\theta\ \Gamma \approx (\Omega_2/\delta_2)^2\Gamma$ and $\Gamma_{|3'\rangle} \sim \cos^2\theta\ \Gamma \approx \Gamma$ (assuming $\Omega_2 < \delta_2$). State $|2'\rangle$ has a linewidth narrower than $\Gamma$ by a factor $(\Omega_2/\delta_2)^2$, which gives rise to the subnatural linewidth structures seen in the temperature vs relative detuning plot (Fig. 4). The other bright state, $|3'\rangle$, has a linewidth similar to the linewidth of the excited state $|3\rangle$.

Thus the interaction of the two laser beams with the three-level atoms results in three new perturbed energy levels and eigenstates. The resonance in the light scattering would produce a similar resonance in the cooling process, which can be used to explain the features of Figs. 4 and 5.

However, in the case of $^{39}$K, optimal cooling occurs for $(\Omega_1/\Omega_2)^2 \approx 3.5$ (see Fig. 7). Thus the bright state shown in Eq. (3) is strictly not valid due to mixing from state $|1\rangle$. However, the dark state given by Eq. (2) can still form. A quantitatively precise explanation for the observed cooling phenomena is provided by calculating the force on the atoms which can be obtained by solving the optical Bloch equations (OBEs) for the three-level system. In order to solve the OBEs we will use the method of continuous fractions developed in [14,20] for a three-level Λ system. A similar analysis has also been done in the case of $D_1$ sub-Doppler cooling of $^7$Li [10]. The optical field as seen by the atom can be written in the form [14]

$$\vec{E} = \hat{e}[E_1 \cos(\omega_1 t)\cos(k_1 z) + E_2 \cos(\omega_2 t)\cos(k_2 z + \phi)], \tag{4}$$

where $\hat{e}$ is the polarization unit vector and $E_i$,$\omega_i$, and $k_i$ ($i = 1,2$) are the electric field intensity, angular frequency resonant to the transitions $|i\rangle \rightarrow |3\rangle$, and corresponding wave vectors, respectively. Here $\phi$ is the phase difference between waves $\omega_1$ and $\omega_2$.

The force on the atoms (in one dimension) in the presence of a bichromatic beam in the case of a three-level Λ system is given by

$$\begin{aligned} F = {} & -\hbar k[\Omega_1(\rho_{13} + \rho_{31})\sin(kz) \\ & + \Omega_2(\rho_{23} + \rho_{32})\sin(kz + \phi)], \end{aligned} \tag{5}$$

where we have assumed that the wave vectors are equal, i.e., $k_1 = k_2 = k$. $\rho_{ij}(i,j = 1,2,3; i \neq j)$ are the coherence terms of the density matrix $\rho$.

The elements of the density matrix $\rho_{ij}$ can be expressed in terms of its Fourier components:

$$\rho_{lj} = \sum_{n=-\infty}^{n=+\infty} \rho_{lj}^{(n)} e^{inkz}. \tag{6}$$

The average force on the atoms is determined by the first nonoscillating term of the Fourier components, and hence the average force on the atom computed over one wavelength can be written as [21]

$$\begin{aligned} F = {} & \frac{i\hbar k}{2}\left\{\Omega_1\left(\rho_{31}^{(-1)} + \rho_{13}^{(-1)} - \rho_{31}^{(1)} - \rho_{13}^{(1)}\right)\right. \\ & + \Omega_2\left[\left(\rho_{32}^{(-1)} + \rho_{23}^{(-1)}\right)\exp(i\phi)\right. \\ & \left.\left. - \left(\rho_{32}^{(1)} + \rho_{23}^{(1)}\right)\exp(-i\phi)\right]\right\}. \end{aligned} \tag{7}$$

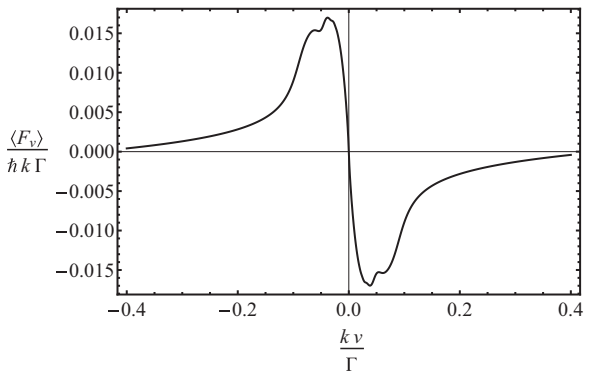


FIG. 9. Force on atoms averaged over the phase $\phi$ as a function of velocity of the atoms for the parameters $\Omega_1 = 0.7\Gamma$, $\Omega_2 = 1.2\Gamma$, and $\delta_1 = \delta_2 = 5\Gamma$.

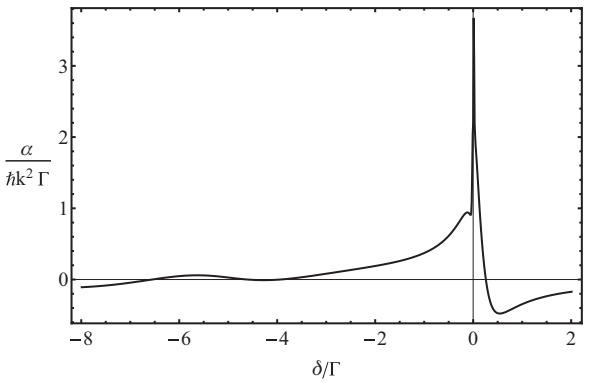


FIG. 10. Coefficient of viscosity $\alpha$ as a function of relative detuning $\delta$. The parameters for the plot are $\Omega_1 = 0.7\gamma$, $\Omega_2 = 1.2\Gamma$, $\delta_2 = 5\Gamma$, and $\phi = 0$.

Using the method of continued fractions, we can now calculate the force on the atoms to arbitrary accuracy using parameters relevant to our experiment. Figure 9 shows the force on an atom as a function of velocity. We calculate the force, taking into account that the relative phase $\phi$ between the two light beams might undergo random changes on time scales of a few milliseconds. The force is thus calculated by averaging over the phase $\phi$ between the two wave vectors, $k_1$ and $k_2$, over the range $(0,2\pi)$ [10]:

$$\langle F_v \rangle = \frac{1}{2\pi} \int_0^{2\pi} F_v d\phi. \tag{8}$$

The force, as we can see, produces effective cooling in a very narrow range of velocities in the Raman condition, i.e., when $\delta_1 = \delta_2 = \delta$. Precooling thus helps and it is indeed necessary to prevent loss of atoms during the $D_1$ molasses cooling phase. Since the atoms in our experiment are already cooled down to about 40 $\mu K$ (which corresponds to $kv/\Gamma \sim 0.02$) prior to the $D_1$ molasses stage, the loss of atoms is minimized. In fact we see that more than 90% of the atoms are captured and cooled. Atoms with velocities significantly higher than the capture velocity of the force would undergo heating and would be lost.

From Fig. 9, we can see that the force is linear for small velocities $v$. The force $F$ around $v = 0$ can be written as

$$F = -\alpha v, \tag{9}$$

where $\alpha$ is the coefficient of viscosity. When $\alpha > 0$, the force is opposite to the direction of velocity, and we expect the atoms to cool; if $\alpha < 0$, the force is in the same direction as that of the velocity, and we expect heating to occur. In Fig. 10 we plot the coefficient of viscosity as a function of the relative detuning ($\delta = \delta_1 - \delta_2$) of the repump beam. The coefficient of viscosity $\alpha$ is obtained from the linear fit of force around $v = 0$. Figure 10 shows the variation of the coefficient of viscosity with relative detuning for the case $\Omega_2^2/\Omega_1^2 > 1$, i.e., $I_C/I_R > 1$. The cooling is maximum when the Raman condition is satisfied (when $\alpha$ is large and positive). As the relative detuning is increased, $\alpha$ becomes negative, and we expect to observe heating around this region. Thus, as seen in Fig. 4, when we start moving from $\delta = 0$ (where the minimum temperature is attained) towards $\delta > 0$, a large increase in temperature can be seen. When the ratio of intensities of the cooling and repumping beams is inverted, i.e., $\Omega_2^2/\Omega_1^2 < 1$ or $I_C/I_R < 1$, the temperature is minimum as enhanced cooling occurs at the Raman resonance (when $\alpha > 0$ and maximum). However, from our model, now we expect resonant heating for negative values of the relative detuning $\delta$ due to the reversal of the roles of the driving laser fields. This is exactly what is observed in Fig. 5, where resonant heating with a subnatural linewidth takes place when $\delta < 0$, near the Raman resonance.

In the model that we have chosen, the coefficient of viscosity becomes negative when the detuning is negative, i.e., the force is in the same direction as the velocity of the atoms, and this should lead to heating of the cloud of atoms (see Fig. 11). This is confirmed by data for $\Delta < 0$ relative to $F' = 2$ as long as the magnitude of the detuning from $F' = 1$ is much larger than the detuning from $F' = 2$. As we go below the resonance of the $\Lambda$ system under consideration, the other $\Lambda$ configuration that is present in our system but has not been considered in our model will start contributing to the total scattering. The second $\Lambda$ system is formed by the transitions $F = 1 \rightarrow F' = 1$ and $F = 2 \rightarrow F' = 1$. In order to understand the effect of the second $\Lambda$ system, we treat both $\Lambda$ systems as independent

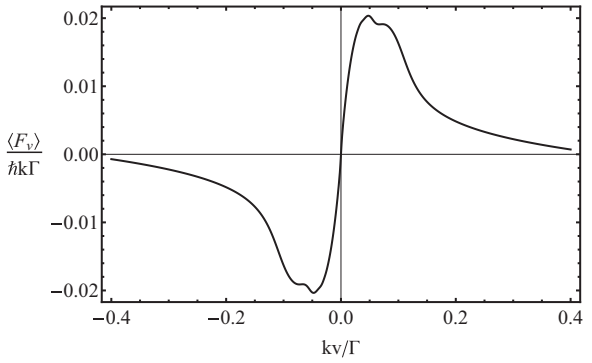


FIG. 11. Force on atoms averaged over the phase $\phi$ as a function of velocity of the atoms for the parameters $\Omega_1 = 0.7\Gamma$, $\Omega_2 = 1.2\Gamma$, and $\delta_1 = \delta_2 = -4\Gamma$.

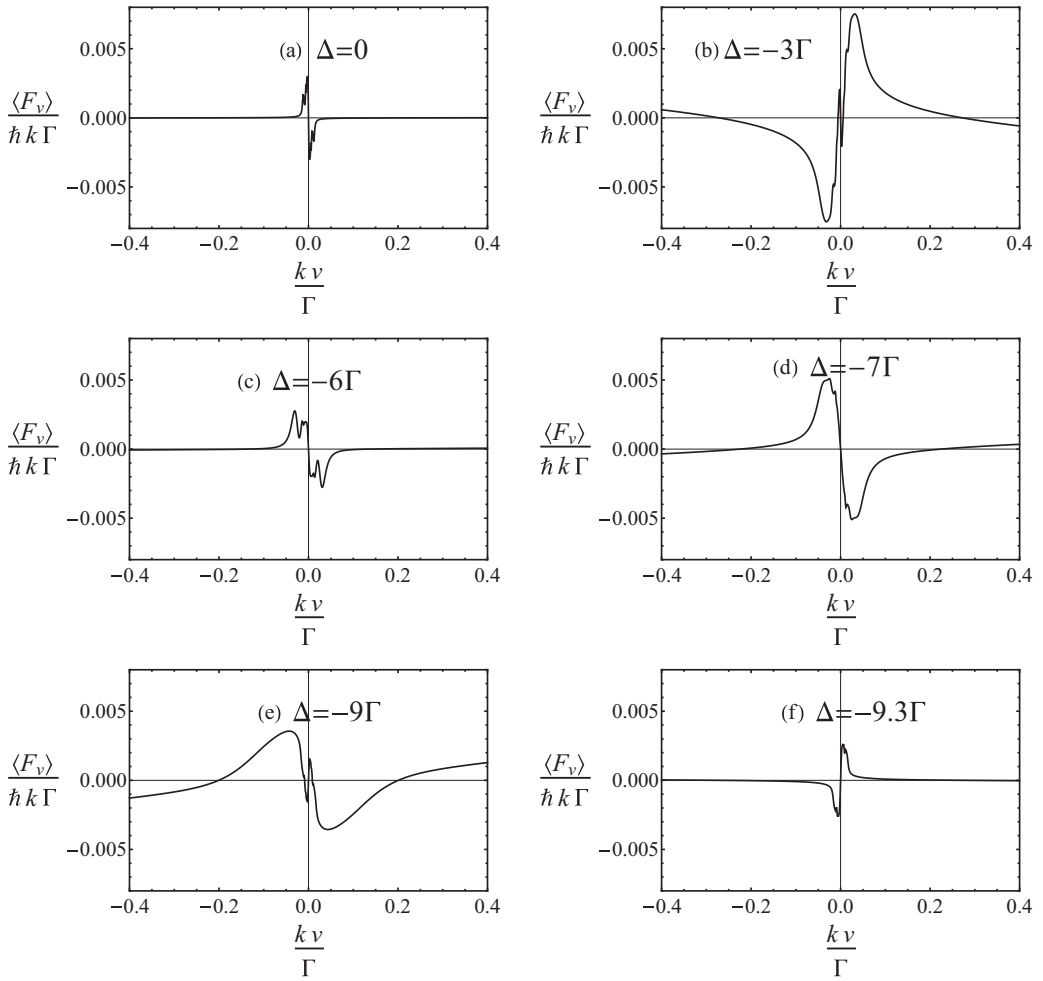


FIG. 12. Force for several cases of absolute negative detuning $\Delta$. Here $\Delta = \delta_1 = \delta_2$. (a) corresponds to $F' = 2$ resonance, and ($f$) corresponds to $F' = 1$ resonance.

entities, taking into account the relative transition strength of individual transitions in their respective Rabi frequencies. With this assumption, we can calculate the force on the atom due to the presence of each $\Lambda$ system and then add the forces obtained individually.

Although simple addition of the two forces is an approximation, the features seen can give us insights about the nature of the forces on the atom when both the $\Lambda$ systems actively participate in the cooling process. In a single absorption-emission cycle only one of the two $\Lambda$ systems present will participate and the force is calculated by averaging over one wavelength and the phase $\phi$. Figure 12(a) corresponds to $\Delta = 0$, where the contribution to the force is entirely due to the presence of the second $\Lambda$ system. When the laser frequency is red detuned by a small amount with respect to $F' = 2$, strong heating occurs, as expected [see Fig. 12(b)]. As the laser frequency is further detuned, heating dominates until $\Delta > -5\Gamma$. At about $\Delta = -6\Gamma$ [see Fig. 12(c)], the slope of the total force starts to become negative for a narrow velocity range, leading to reduced heating. Blue Sisyphus cooling relative to $F' = 1$ eventually overwhelms the heating from red detuning relative to $F' = 2$, and we recover low temperature in the molasses for a small range of detuning. Closer to the $F' = 1$ transition, the cooling reduces again for $\Delta < -9\Gamma$ before it completely converts to heating at the $F' = 1$ resonance. Hence most features observed in Fig. 6 are explained by our model involving two $\Lambda$ systems.

## IV. CONCLUSION

We have explored and established quantum coherent dark-state-enhanced cooling of $^{39}$K atoms in a three-level $\Lambda$ configuration over a wide range of parameters. A plausible theoretical framework to analyze results on sub-Doppler cooling is presented which explains most of the observed features. Sisyphus cooling of the atoms in the periodic potential humps created by the laser beams detuned to the blue side of the $D_1$ transition and reduced scattering after they get trapped in the dark state formed at Raman resonance in the $\Lambda$ configuration are the main physical features of the enhanced cooling. Calculations show that the cooling happens for a narrow velocity class of atoms, making it essential to precool the atoms to temperatures below 100 $\mu$K to avoid atom loss. We achieve this by implementing a standard $D_2$-molasses scheme prior to the molasses in the Raman configuration using the $D_1$ levels. The two-stage sub-Doppler cooling in molasses of $^{39}$K results in a significant decrease in temperature to about 12 $\mu$K, corresponding to a phase-space density

$>2 \times 10^{-5}$. Thus the atomic cloud is well suited for transfer to magnetic or optical traps for further cooling to quantum degeneracy.

**ACKNOWLEDGMENT**

We thank Dr. Thomas Bourdel, Institut d' Optique, Paris, for discussions and for pointing out an important correction.

[1] G. Modugno, G. Ferrari, G. Roati, R. J. Brecha, A. Simoni, and M. Inguscio, Science **294**, 1320 (2001).
[2] G. Roati, M. Zaccanti, C. D'Errico, J. Catani, M. Modugno, A. Simoni, M. Inguscio, and G. Modugno, Phys. Rev. Lett. **99**, 010403 (2007).
[3] C. D'Errico, M. Zaccanti, M. Fattori, G. Roati, M. Inguscio, G. Modugno, and A. Simoni, New J. Phys. **9**, 223 (2007).
[4] C. Fort, A. Bambini, L. Cacciapuoti, F. S. Cataliotti, M. Prevedelli, G. M. Tino, and M. Inguscio, Eur. Phys. J. D **3**, 113 (1998).
[5] V. Gokhroo, G. Rajalakshmi, R. Kollengode Easwaran, and C. S. Unnikrishnan, J. Phys. B **44**, 115307 (2011).
[6] M. Landini, S. Roy, L. Carcagní, D. Trypogeorgos, M. Fattori, M. Inguscio, and G. Modugno, Phys. Rev. A **84**, 043432 (2011).
[7] A. Hemmerich, M. Weidemüller, T. Esslinger, C. Zimmermann, and T. Hänsch, Phys. Rev. Lett. **75**, 37 (1995).
[8] D. Boiron, C. Triché, D. R. Meacher, P. Verkerk, and G. Grynberg, Phys. Rev. A **52**, R3425 (1995).
[9] D. Rio Fernandes, F. Sievers, N. Kretzschmar, S. Wu, C. Salomon, and F. Chevy, Europhys. Lett. **100**, 63001 (2012).
[10] A. T. Grier, I. Ferrier-Barbut, B. S. Rem, M. Delehaye, L. Khaykovich, F. Chevy, and C. Salomon, Phys. Rev. A **87**, 063411 (2013).
[11] A. Aspect, E. Arimondo, R. Kaiser, N. Vansteenkiste, and C. Cohen-Tannoudji, Phys. Rev. Lett. **61**, 826 (1988).
[12] P. M. Duarte, R. A. Hart, J. M. Hitchcock, T. A. Corcovilos, T.-L. Yang, A. Reed, and R. G. Hulet, Phys. Rev. A **84**, 061406 (2011).
[13] A. Bambini and A. Agresti, Phys. Rev. A **56**, 3040 (1997).
[14] D. V. Kosachev and Y. V. Rozhdestvenskii, Sov. J. Exp. Theor. Phys. **79**, 856 (1994), http://www.jetp.ac.ru/cgi-bin/dn/e_079_06_0856.pdf.
[15] B. Lounis and C. Cohen-Tannoudji, J. Phys. II **2**, 579 (1992).
[16] C. G. Townsend, N. H. Edwards, C. J. Cooper, K. P. Zetie, C. J. Foot, A. M. Steane, P. Szriftgiser, H. Perrin, and J. Dalibard, Phys. Rev. A **52**, 1423 (1995).
[17] M. Weidemüller, T. Esslinger, M. A. Ol'Shanii, A. Hemmerich, and T. W. Hänsch, Europhys. Lett. **27**, 109 (1994).
[18] M. Fleischhauer, A. Imamoglu, and J. P. Marangos, Rev. Mod. Phys. **77**, 633 (2005).
[19] C. Cohen-Tannoudji, J. Dupont-Roc, and G. Grynberg, *Atom-Photon Interactions: Basic Processes and Applications* (Wiley Interscience, New York, 1992).
[20] V. S. Letokhov and V. G. Minogin, Phys. Rep. **73**, 1 (1981).
[21] D. V. Kosachiov, Y. V. Rozhdestvensky, and G. Nienhuis, J. Opt. Soc. Am. B **14**, 535 (1997).